A Comparative study on structural, morphological and photocatalytic properties of anodically grown ZnO nanowires under varying parameters

Erdem Tevfik Ozdemir
Dokuz Eylul University: Dokuz Eylul Universitesi
Uğur KARTAL (ugurkartal@iyte.edu.tr)
Dokuz Eylul Universitesi Muhendislik Fakultesi https://orcid.org/0000-0002-5557-2300
Tuncay Dikici
Dokuz Eylul University: Dokuz Eylul Universitesi
Mustafa Erol
Dokuz Eylul University: Dokuz Eylul Universitesi
Metin Yurddaskal
Dokuz Eylul University: Dokuz Eylul Universitesi

Research Article

Keywords: Nanowire, photocatalyst, degradation, ZnO, anodization

Posted Date: May 4th, 2021

DOI: https://doi.org/10.21203/rs.3.rs-479424/v1

Version of Record: A version of this preprint was published at Journal of Materials Science: Materials in Electronics on September 29th, 2021. See the published version at https://doi.org/10.1007/s10854-021-07115-7.

A Comparative study on structural, morphological and photocatalytic properties of anodically grown ZnO nanowires under varying parameters

Erdem Tevfik Ozdemir[1], Ugur Kartal[2*], Tuncay Dikici[3,4], Mustafa Erol[4,5], Metin Yurddaskal[5]

[1]The Graduate School of Natural and Sciences, Dokuz Eylul University, Izmir, Turkey

[2]Department of Materials Science and Engineering, Izmir Institute of Technology, Izmir, Turkey

[3]Torbali Vocational School, Dokuz Eylul University, Izmir, Turkey

[4]Center for Fabrication and Application of Electronic Materials, Dokuz Eylul University, Izmir, Turkey

[5]Department of Metallurgical and Materials Engineering, Dokuz Eylul University, Izmir, Turkey

Abstract

In this study, Zinc oxide (ZnO) nanowires (NWs) were successfully produced on Zn plates through electrochemical anodization in potassium bicarbonate aqueous electrolytes with different production parameters in two groups as applied voltage and anodization time. Subsequently, the ZnO NWs were annealed at 300 ℃ for 1 h in air atmosphere to increase crystallinity and remove organic residues. Structural and morphological properties were determined through X-ray diffraction (XRD) and scanning electron microscopy (SEM) analysis. The effect of anodization parameters on the structure of ZnO NWs and thus their photocatalytic activities were evaluated in detail by UV spectrophotometer. The results pointed out that, the most effective nanostructure on the photocatalytic degradation of methylene blue was obtained at the sample anodized under 30 V for 30 min at room temperature with 90.6% degradation efficiency among the samples. This result shows that the NW structured ZnO materials are promising to be used as effective photocatalysts in the removal of organic pollutants by solar energy and their conversion to green compounds.

Keywords: Nanowire, photocatalyst, degradation, ZnO, anodization

Corresponding Author: ugurkartal@iyte.edu.tr (Ugur KARTAL)

1 Introduction

Semiconductors are environmentally friendly materials that have a wide range of daily applications and do not pose major environmental risks. The metal oxide semiconductors (ZnO, TiO_2, Fe_2O_3, CuO, NiO, etc.), have favorable properties that desired in a variety of applications [1]. One of these applications is photocatalysis and some semiconductors, such as TiO_2 and ZnO, are heavily utilized for the degradation of environmental contaminants [2–5]. Photocatalysis, also known as photo-assisted catalysis, has processes similar to photosynthesis [3]. When photons with energies greater than the band gap energy of the photocatalyst are absorbed, at least two reactions occur simultaneously and carbon dioxide and water come out of dissolution of various organic compounds [6]. After publication of Fujishima and Honda on photocatalytic water splitting via TiO_2 in 1972, studies on TiO_2 as a photocatalyst have increased considerably [7]. Although the TiO_2 photocatalyst is widely used, ZnO is a feasible alternative to be photocatalyst because of its band gap energy and its relatively lower cost of production [8,9].

ZnO is a n-type semiconductor that has been receiving a great attention in the last decade [5]. ZnO, with a wide band gap (3.37 eV) and large exciton binding energy (60 meV) [10–13], has found a wide range of possible applications in photocatalysis [14], photovoltaics [15], light-emitting diodes [16], sensing [17] and many others [18].

One-dimensional (1D) nanostructures have been studied affluently due to their high charge transport efficiency and surface to volume ratio [19]. ZnO nanowires (NWs) is the most engaging nanostructures of ZnO. Up to now, several different synthesis methods to fabricate ZnO NWs have been used in the literature, e.g., hydrothermal methods [20], chemical vapor deposition [21], template-directed methods [22], sol-gel [11], molecular beam epitaxy [23], atomic layer deposition [24], pulsed laser deposition [25], or direct precipitation [26]. Nonetheless, most of these methods required long reaction times, expensive experimental setups and complicated procedures.

Apart from aforementioned methods, electrochemical anodization is a promising method as efficient, highly controllable, fast and cost effective. This process has gained much attention after demonstration of two-step approach by Masuda and Fukuda in 1995 [27]. The oxidizing of a surface of an anode metal is provided through electrochemical anodization method, in a specific electrolyte under a specific voltage at room temperature, resulting in the formation of various nanostructured materials e.g., nanoporous-like structures, nanoflakes, nanoflowers, nanoneedles and NWs [1,28,29]. It is obvious that bicarbonate solutions are very popular electrolytes for anodizing of Zn to obtain ZnO NWs [30]. The conditions such as applied during

anodic oxidation, including electrolyte concentration, applied potential, temperature and duration of the process, have a profound effect on the physical and chemical properties of the NWs [12].

In this context, ZnO NWs have been prepared on Zn plate by electrochemical anodizing technique under different production parameters such as applied voltage and anodization time. The phase structures, surface morphologies and photocatalytic activities of ZnO NWs were examined in detail.

2 Experimental studies

2.1 Materials

Zn plate (99.9%, thickness 1 mm) was supplied by BByes Store. Potassium bicarbonate ($KHCO_3$, 99.7%), absolute ethanol (C_2H_5OH, ≥99.9), isopropyl alcohol (C_3H_8O, 99.5%) were supplied from Merck and used as purchased.

2.2 Synthesis of ZnO NWs

Anodization samples of 25x25 mm^2 dimensions were cut from Zn plate. Subsequently, the Zn substrates were washed with C_2H_5OH and distilled water in an ultrasonic cleaner (Everest CleanEx-2511) for 15 min, respectively. Cleaned substrates were dried at room temperature in the air atmosphere. Applied anodization parameters to the Zn substrates were categorized and listed in Table 1. Anodization was performed under different voltages (10-40 V) and anodization times (10-120 min) for investigating the anodization parameters on the structure of produced ZnO which has a certain effect on the photocatalytic activity. For anodization process, two-electrode electrochemical cell setup (Fig. 1) containing Zn plate as a working electrode, stainless steel plate as a counter electrode and aqueous solution of $KHCO_3$ (50 mM) as an electrolyte was used. The distance between two electrodes was kept at 10 cm through anodization process. The anodized samples were rinsed with distilled water and C_3H_8O to remove remaining electrolyte, respectively. Afterward, the samples were put in a drying oven (Binder ED53) at 80 °C for 60 min. Finally, the as-anodized samples were annealed at a temperature of 300 °C for 1 h at the heating rate of 2 °C min^{-1} and stored in a desiccator before characterization.

Table 1 Anodization parameters of ZnO NWs

Group	Sample Code	Voltage (V)	Time (min)
Group 1	S1	10	30
	S2	20	30
	S3	30	30
	S4	40	30
Group 2	S5	10	10
	S6	10	20
	S7	10	60
	S8	10	120

2.3 Materials Characterization

In order to elucidate the phase structure, as-anodized and annealed samples were examined by an X-ray diffractometer (XRD, Thermo Scientific ARL X'TRA) with a Cu-Kα (1.54185 Å) irradiation in the range of 2θ = 10-90° at the scan rate of 2 °/min. The surface morphology and nanostructure of the samples were observed by a scanning electron microscope (SEM, Carl Zeiss 300VP).

2.4 Photocatalytic Measurements

The photocatalytic activities of the samples were scrutinized by using 10^{-5} M of methylene blue (MB) solution under 300W Osram Ultra-Vitalux E27 (4.53% UVA, 1% UVB, 94.47% Vis) light source at room temperature. In order to compare catalyst-free degradation of MB under irradiation a reference solution was also prepared. The photocatalysts were immersed into 30 mL of MB aqueous solution in beakers and placed under the light source with a distance approximately 20 cm. In order to determine the absorbencies, 3 ml of the MB solution from each beaker was taken out at given time intervals after UV light exposure. The absorption measurements of the MB solution were performed at the wavelength from 400 nm to 800 nm and confirmed by monitoring the decreasing of absorbance at 664 nm, which is the characteristic peak of MB, by a UV spectrophotometer (Shimadzu UV 1240 spectrophotometer) [31]. Within the scope of Lambert Beer Law, the absorbance values were converted to concentration values [32]. Their photocatalytic degradation efficiency was defined as $[(C_0\text{-}C)/C_0]\times100$ (C_0; initial concentration, C; final concentration). For the final step of characterization, photocatalytic reaction kinetics on MB degradation were calculated for all samples using the catalysts.

3 Results and discussion

3.1 Structural Analysis

The structures of the as-anodized and annealed ZnO NWs were analyzed via the XRD technique. The XRD patterns of ZnO NWs which produced at different voltages and anodization time by electrochemical anodization method were shown in Fig. 2a and 2b for sample groups 1 and 2, respectively. It was observed from these patterns, the samples were mixed form of metallic Zn and wurtzite phases as marked with 1 and 2 for Zn (ICDD 03-065-5973) and wurtzite (ICDD 00-036-1451), respectively [1]. Note that the peaks (1) metallic Zn were arised from Zn substrates in all patterns. As shown in Fig. 2a and 2b, the peak intensities of the ZnO structures were augmented with the rising of applied voltage and anodization time. The structural data of the samples were found to be convenient to the literature [1,10,33].

3.2 Morphological Analysis

Fig. 3 shows the surface images of the ZnO NWs were obtained at different voltages such as 10, 20, 30 and 40 V. As seen in the Fig. 3a, the nanoflower structures formed at an initial point of growth transformed to aligned NW structures. ZnO NWs have become thinner and denser structures with increasing voltage. When the applied voltage is 40 V, there were linked and interpenetrated structures due to the length of the NWs as seen in Fig. 3d. Furthermore, micro cracks were observed on the surface due to oxygen evaluation during anodization at high voltage. Fig. 4 indicates the effects of anodizing time on the morphology of ZnO NWs. The results show that as the anodizing time increases, the thickness of the ZnO NWs decreases while the density increases. The hierarchical ZnO NWs structure has emerged after anodization for 60 min. As seen in literature, these results are in good agreement with the previously published studies [19,28,30].

3.3 Photocatalytic Activity

The photocatalytic mechanism of ZnO NWs with different morphological properties was shown in Fig. 5. Due to the light excitation of ZnO, holes (h^+) are formed in the valence band, while electrons (e^-) are transferred to the conduction band. Thus, when oxygen molecules (O_2) are excited by light, they form super oxide radical anions ($\bullet O_2^-$). These O_2's degrade MB into green compounds such as carbon dioxide (CO_2) and water (H_2O). The reactions that occur during the degradation of MB under UV light source can be listed as follows:

$$ZnO + h\upsilon \longrightarrow ZnO\ (h^+ + e^-) \quad (1)$$

$$O_2 + e^- \longrightarrow \bullet O_2^- \quad (2)$$

$$H_2O + h^+ \longrightarrow \bullet OH + H^+ \quad (3)$$

$$h^+ + \bullet O_2^- + \bullet OH + MB \longrightarrow CO_2 + H_2O \quad (4)$$

The photocatalytic performances of the samples were obtained by measuring the absorbance data of the samples taken from the degraded MB at certain time intervals. The MB aqueous solution under UV-Vis light irradiation is degraded by photocatalysts thanks to the photocatalytic effect. Concentration data were obtained using the Lambert-Beer law from the absorbance values at 664 nm which is the characteristic peak of MB. Fig. 6a shows the change in concentration of MB over 11 hours. The degradation efficiency, kinetic rate constant and determination coefficient parameters of the samples are given in Table 2. The k values obtained from the slope of the lines in Fig. 6b show that the most enhanced photocatalytic degradation of MB was obtained with the S3 sample. The k values obtained showed that the photocatalytic degradation of MB correlated with the anodizing parameters. As the surface morphology and dimensions of the structure change with changing anodizing parameters, the photocatalytic performance also changes in relation to this. The photocatalytic degradation rate was calculated for all samples using Eq. 5:

$$\ln \frac{C_0}{C} = kt \quad (5)$$

where C_0, C and t are the initial concentration of MB, the concentration of MB at certain time and irradiation time, respectively.

Table 2 Photocatalytic parameters of the ZnO NW structured samples

Samples	**Group 1**				**Group 2**				
	Ref.	**S1**	**S2**	**S3**	**S4**	**S5**	**S6**	**S7**	**S8**
Degradation efficiency (%)	21.8	80.4	86.3	90.6	88.3	86.6	84.6	77.9	83.8
Kinetic rate constant (k) ($10^{-3}min^{-1}$)	0.374	2.471	3.015	3.590	3.256	3.047	2.835	2.225	2.765
R^2	0.992	0.992	0.983	0.988	0.994	0.99	0.980	0.996	0.986

Many factors such as nanostructure, surface area, crystallinity, phase composition, crystal orientation and structure dimensions affect photocatalytic performance. The degradation efficiencies of MB with an initial absorbance value of 0.695 at 664 nm by different samples were calculated for each sample. The results obtained are given in Table 2 and shown as a bar graph in Fig. 7. As can be seen from Fig. 7, the degradation efficiency after 11 hours for the arbitration sample is 21.8% while it is 90.6% for the S3 sample. With this degradation efficiency value, the S3 sample has the best photocatalytic performance. It is thought that the reason for the S3 sample having the best photocatalytic activity is that the surface morphology is densely composed of thin and long NW and the high surface area obtained due to the presence of these NWs independently from each other. As a result, photocatalysts with different photocatalytic activity values can be obtained by controlling the anodization time and voltage, which have significant effects on the surface area.

Absorption spectra of MB for sample S3 were drawn for different durations and are shown in Fig. 8. MB was degraded under UV-Vis light source using S3 sample for 11 hours. The absorbance value of MB at 664 nm, which was kept under UV-Vis light illumination for 11 hours, was reduced from 0.695 to 0.065 with the degradation efficiency of 90.6% in the presence of the S3 sample.

4 CONCLUSION

In summary, ZnO NWs were successfully formed on Zn plates using facile electrochemical anodization method in potassium bicarbonate aqueous electrolytes at different anodizing parameters. The structural characteristics of the ZnO NWs can be controlled by various growth parameters. The obtained SEM results reveal that ZnO NWs have become thinner and denser structures with increasing applied voltage and anodization time. Furthermore, cracking on the surfaces happened at voltages over 30 V due to oxygen evolution. In addition to the structural results the hierarchical ZnO NWs structure has emerged after anodization for 60 min. On the basis of these photocatalysts, the highest photocatalytic efficiency with 90.6% belongs to the sample anodized at 30 V for 30 min. This result shows that NW structured ZnO materials are promising that they can be used as effective photocatalysts in the conversion of organic pollutants by solar energy into green compounds.

5 REFERENCES

[1] A. Yavaş, S. Güler, M. Erol, Growth of ZnO nanoflowers: effects of anodization time

and substrate roughness on structural, morphological, and wetting properties, J. Aust. Ceram. Soc. 56 (2020) 995–1003. https://doi.org/10.1007/s41779-019-00440-5.

[2] M. Erol, T. Dikici, M. Toparli, E. Celik, The effect of anodization parameters on the formation of nanoporous TiO_2 layers and their photocatalytic activities, J. Alloys Compd. 604 (2014) 66–72. https://doi.org/10.1016/j.jallcom.2014.03.105.

[3] D.F. Ollis, Photocatalytic purification and remediation of contaminated air and water, Comptes Rendus l'Academie Des Sci. - Ser. IIc Chem. 3 (2000) 405–411. https://doi.org/10.1016/S1387-1609(00)01169-5.

[4] R.Y. Hong, J.H. Li, L.L. Chen, D.Q. Liu, H.Z. Li, Y. Zheng, J. Ding, Synthesis, surface modification and photocatalytic property of ZnO nanoparticles, Powder Technol. 189 (2009) 426–432. https://doi.org/10.1016/j.powtec.2008.07.004.

[5] K.M. Lee, C.W. Lai, K.S. Ngai, J.C. Juan, Recent developments of zinc oxide based photocatalyst in water treatment technology: A review, Water Res. 88 (2016) 428–448. https://doi.org/10.1016/j.watres.2015.09.045.

[6] A. Fujishima, X. Zhang, D.A. Tryk, TiO_2 photocatalysis and related surface phenomena, Surf. Sci. Rep. 63 (2008) 515–582. https://doi.org/10.1016/j.surfrep.2008.10.001.

[7] A. Fujishima, K. Honda, Electrochemical photolysis of water at a semiconductor electrode, Nature. 238 (1972) 37–38. https://doi.org/10.1038/238037a0.

[8] D.M. Fouad, M.B. Mohamed, Comparative study of the photocatalytic activity of semiconductor nanostructures and their hybrid metal nanocomposites on the photodegradation of malathion, J. Nanomater. 2012 (2012). https://doi.org/10.1155/2012/524123.

[9] Y.J. Jang, C. Simer, T. Ohm, Comparison of zinc oxide nanoparticles and its nano-crystalline particles on the photocatalytic degradation of methylene blue, Mater. Res. Bull. 41 (2006) 67–77. https://doi.org/10.1016/j.materresbull.2005.07.038.

[10] Z. Hu, Q. Chen, Z. Li, Y. Yu, L.M. Peng, Large-scale and rapid synthesis of ultralong ZnO nanowire films via anodization, J. Phys. Chem. C. 114 (2010) 881–889. https://doi.org/10.1021/jp9094744.

[11] S.E. Ahn, J.L. Soo, H. Kim, S. Kim, B.H. Kang, K.H. Kim, G.T. Kim, Photoresponse of sol-gel-synthesized ZnO nanorods, Appl. Phys. Lett. 84 (2004) 5022–5024. https://doi.org/10.1063/1.1763633.

[12] L. Zaraska, K. Mika, K. Syrek, G.D. Sulka, Formation of ZnO nanowires during anodic oxidation of zinc in bicarbonate electrolytes, J. Electroanal. Chem. 801 (2017) 511–520. https://doi.org/10.1016/j.jelechem.2017.08.035.

[13] J. Dong, Z. Liu, J. Dong, D. Ariyanti, Z. Niu, S. Huang, W. Zhang, W. Gao, Self-organized ZnO nanorods prepared by anodization of zinc in NaOH electrolyte, RSC Adv. 6 (2016) 72968–72974. https://doi.org/10.1039/c6ra16995c.

[14] C. Tian, Q. Zhang, A. Wu, M. Jiang, B. Jiang, H. Fu, Cost-effective large-scale synthesis of ZnO photocatalyst with excellent performance for dye photodegradation, Chem. Commun. 48 (2012) 2858–2860. https://doi.org/10.1039/c2cc16434e.

[15] R. Kumar, A. Umar, G. Kumar, H.S. Nalwa, A. Kumar, M.S. Akhtar, Zinc oxide nanostructure-based dye-sensitized solar cells, J. Mater. Sci. 52 (2017) 4743–4795. https://doi.org/10.1007/s10853-016-0668-z.

[16] A. Achour, M.A. Soussou, K. Ait Aissa, M. Islam, N. Barreau, E. Faulques, L. Le Brizoual, M.A. Djouadi, M. Boujtita, Nanostructuration and band gap emission enhancement of ZnO film via electrochemical anodization, Thin Solid Films. 571 (2014) 168–174. https://doi.org/10.1016/j.tsf.2014.10.061.

[17] N. Tiwale, Zinc oxide nanowire gas sensors: Fabrication, functionalisation and devices, Mater. Sci. Technol. (United Kingdom). 31 (2015) 1681–1697. https://doi.org/10.1179/1743284714Y.0000000747.

[18] Y. Zhang, M.K. Ram, E.K. Stefanakos, D.Y. Goswami, Synthesis, characterization, and applications of ZnO nanowires, J. Nanomater. (2012). https://doi.org/10.1155/2012/624520.

[19] A. Mateen Tantray, M.A. Shah, Photo electrochemical ability of dense and aligned ZnO nanowire arrays fabricated through electrochemical anodization, Chem. Phys. Lett. 747 (2020) 137346. https://doi.org/10.1016/j.cplett.2020.137346.

[20] J.Y. Kim, J.W. Cho, S.H. Kim, The characteristic of the ZnO nanowire morphology grown by the hydrothermal method on various surface-treated seed layers, Mater. Lett. 65 (2011) 1161–1164. https://doi.org/10.1016/j.matlet.2010.10.092.

[21] J.L. Yang, S.J. An, W. Il Park, G.C. Yi, W. Choi, Photocatalysis using ZnO thin films and nanoneedles grown by metal-organic chemical vapor deposition, Adv. Mater. 16 (2004) 1661–1664. https://doi.org/10.1002/adma.200306673.

[22] Y.H. Chen, Y.M. Shen, S.C. Wang, J.L. Huang, Fabrication of one-dimensional ZnO nanotube and nanowire arrays with an anodic alumina oxide template via electrochemical deposition, Thin Solid Films. 570 (2014) 303–309. https://doi.org/10.1016/j.tsf.2014.03.014.

[23] A. Menzel, K. Subannajui, R. Bakhda, Y. Wang, R. Thomann, M. Zacharias, Tuning the growth mechanism of ZnO nanowires by controlled carrier and reaction gas modulation

in thermal CVD, J. Phys. Chem. Lett. 3 (2012) 2815–2821. https://doi.org/10.1021/jz301103s.

[24] K. Subannajui, F. Güder, J. Danhof, A. Menzel, Y. Yang, L. Kirste, C. Wang, V. Cimalla, U. Schwarz, M. Zacharias, An advanced fabrication method of highly ordered ZnO nanowire arrays on silicon substrates by atomic layer deposition, Nanotechnology. 23 (2012) 7. https://doi.org/10.1088/0957-4484/23/23/235607.

[25] C. Florica, N. Preda, A. Costas, I. Zgura, I. Enculescu, ZnO nanowires grown directly on zinc foils by thermal oxidation in air: Wetting and water adhesion properties, Mater. Lett. 170 (2016) 156–159. https://doi.org/10.1016/j.matlet.2016.02.035.

[26] J. Huang, H. Ren, P. Sun, C. Gu, Y. Sun, J. Liu, Facile synthesis of porous ZnO nanowires consisting of ordered nanocrystallites and their enhanced gas-sensing property, Sensors Actuators, B Chem. 188 (2013) 249–256. https://doi.org/10.1016/j.snb.2013.06.103.

[27] H. Masuda, K. Fukuda, Ordered metal nanohole arrays made by a two-step replication of honeycomb structures of anodic alumina, Science (80-.). 268 (1995) 1466–1468. https://doi.org/10.1126/science.268.5216.1466.

[28] D.O. Miles, P.J. Cameron, D. Mattia, Hierarchical 3D ZnO nanowire structures via fast anodization of zinc, J. Mater. Chem. A. 3 (2015) 17569–17577. https://doi.org/10.1039/c5ta03578c.

[29] A. Ramirez-canon, D.O. Miles, J. Cameron, D. Mattia, Zinc oxide nanostructured films via anodization : a rational design approach †, (2013) 25323–25330. https://doi.org/10.1039/c3ra43886d.

[30] L. Zaraska, K. Mika, M. Zych, G.D. Sulka, Anodic formation of zinc oxide nanostructures with various morphologies, INC, 2020. https://doi.org/10.1016/b978-0-12-816706-9.00012-1.

[31] M.U. Anu Prathap, B. Kaur, R. Srivastava, Hydrothermal synthesis of CuO micro-/nanostructures and their applications in the oxidative degradation of methylene blue and non-enzymatic sensing of glucose/H_2O_2, J. Colloid Interface Sci. 370 (2012) 144–154. https://doi.org/10.1016/j.jcis.2011.12.074.

[32] S. Demirci, T. Dikici, M. Yurddaskal, S. Gultekin, M. Toparli, E. Celik, Synthesis and characterization of Ag doped TiO_2 heterojunction films and their photocatalytic performances, Appl. Surf. Sci. 390 (2016) 591–601. https://doi.org/10.1016/j.apsusc.2016.08.145.

[33] Y.T. Kim, J. Park, S. Kim, D.W. Park, J. Choi, Fabrication of hierarchical ZnO

nanostructures for dye-sensitized solar cells, Electrochim. Acta. 78 (2012) 417–421. https://doi.org/10.1016/j.electacta.2012.06.022.

Figures

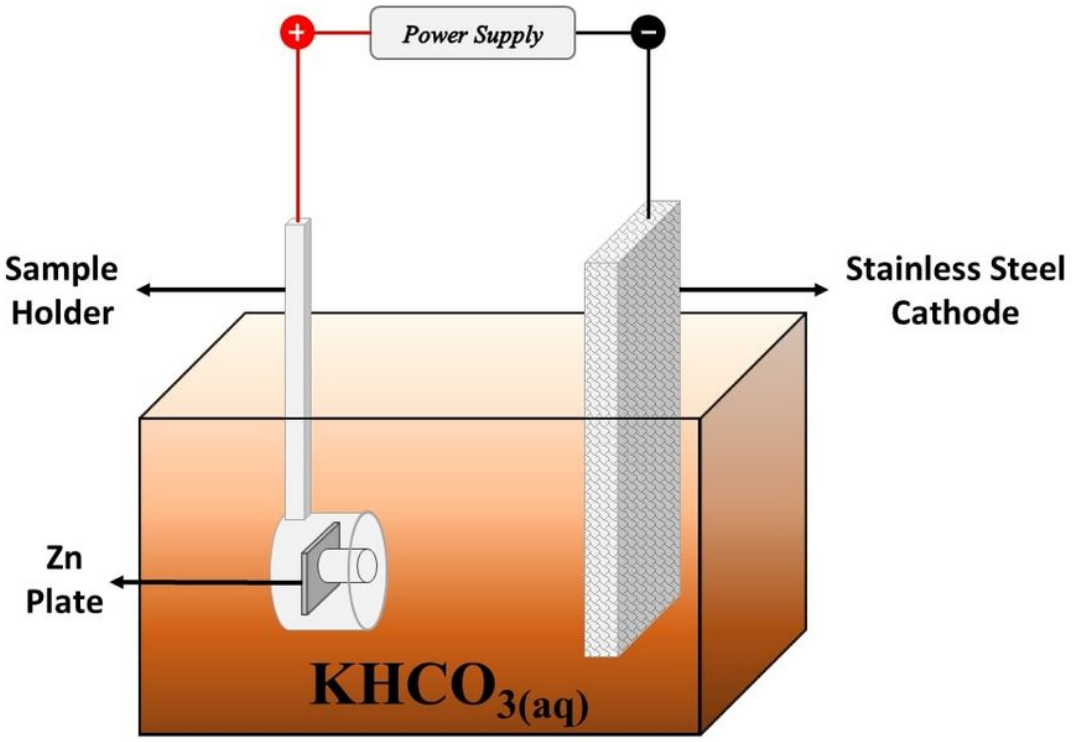

Figure 1

For anodization process, two-electrode electrochemical cell setup (Fig. 1) containing Zn plate as a working electrode, stainless steel plate as a counter electrode and aqueous solution of KHCO3 (50 mM) as an electrolyte was used.

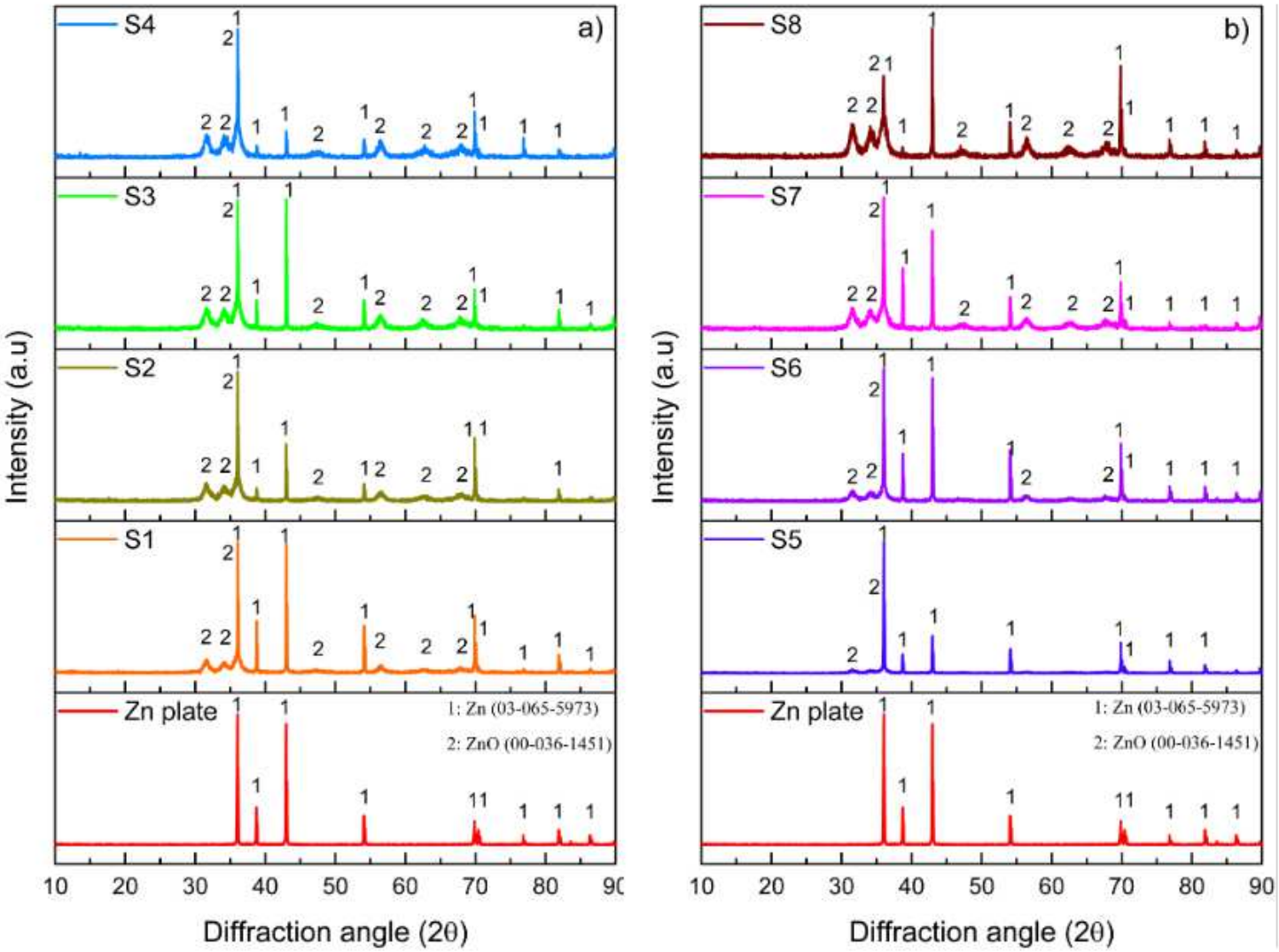

Figure 2

As shown in Fig. 2a and 2b, the peak intensities of the ZnO structures were augmented with the rising of applied voltage and anodization time.

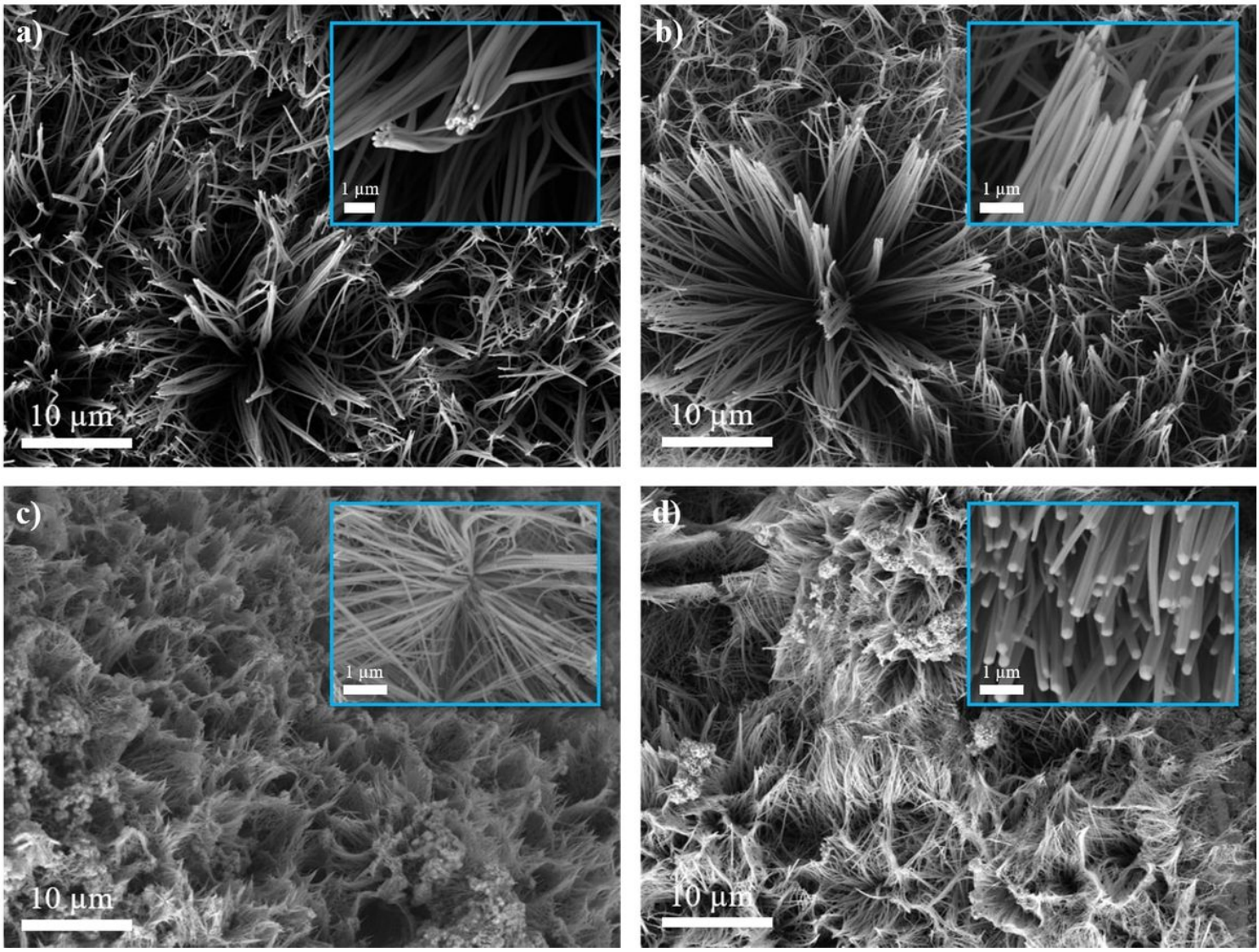

Figure 3

Fig. 3 shows the surface images of the ZnO NWs were obtained at different voltages such as 10, 20, 30 and 40 V. As seen in the Fig. 3a, the nanoflower structures formed at an initial point of growth transformed to aligned NW structures. ZnO NWs have become thinner and denser structures with increasing voltage. When the applied voltage is 40 V, there were linked and interpenetrated structures due to the length of the NWs as seen in Fig. 3d. Furthermore, micro cracks were observed on the surface due to oxygen evaluation during anodization at high voltage.

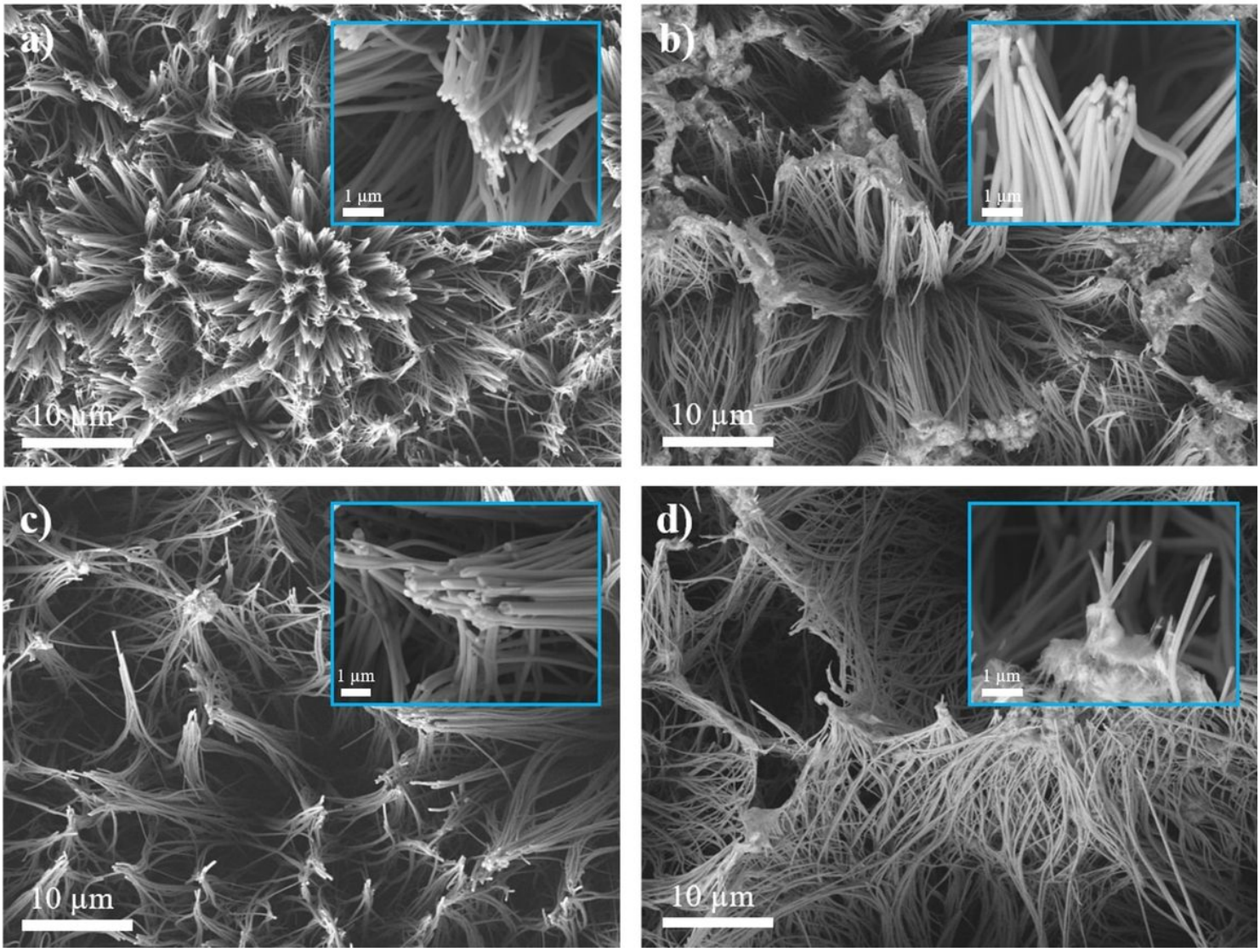

Figure 4

Fig. 4 indicates the effects of anodizing time on the morphology of ZnO NWs. The results show that as the anodizing time increases, the thickness of the ZnO NWs decreases while the density increases. The hierarchical ZnO NWs structure has emerged after anodization for 60 min.

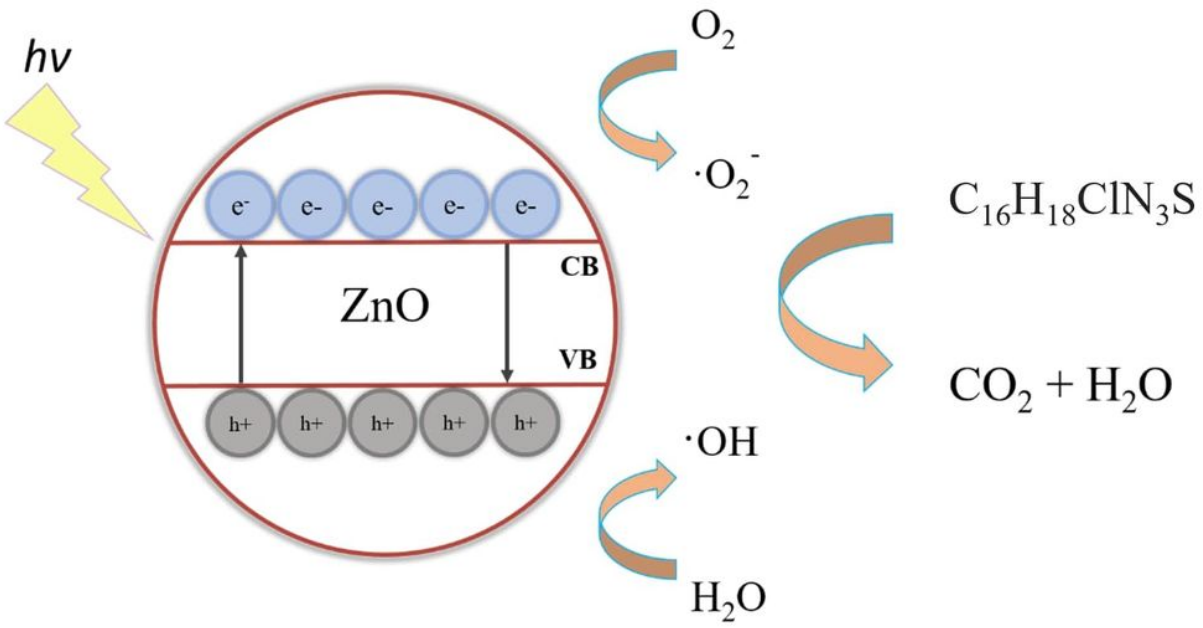

Figure 5

The photocatalytic mechanism of ZnO NWs with different morphological properties was shown in Fig. 5.

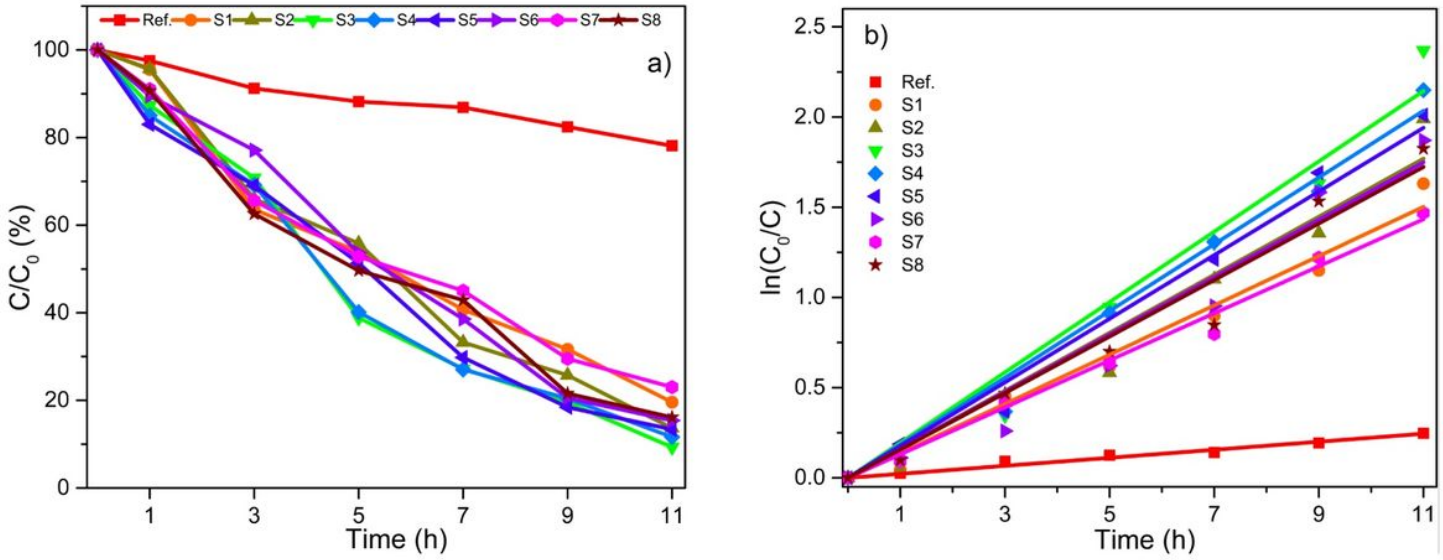

Figure 6

Fig. 6a shows the change in concentration of MB over 11 hours. The degradation efficiency, kinetic rate constant and determination coefficient parameters of the samples are given in Table 2. The k values obtained from the slope of the lines in Fig. 6b show that the most enhanced photocatalytic degradation of MB was obtained with the S3 sample.

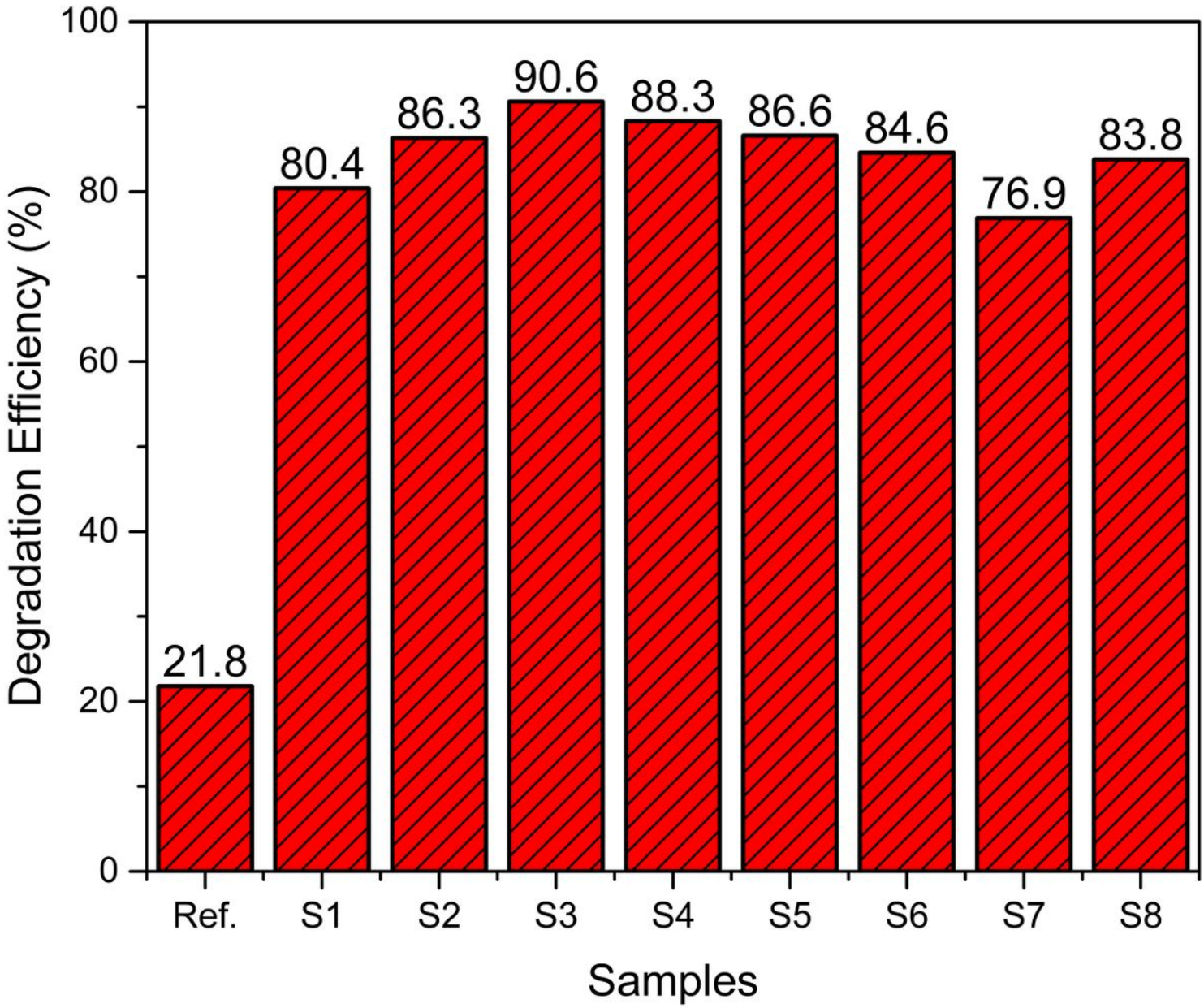

Figure 7

The degradation efficiencies of MB with an initial absorbance value of 0.695 at 664 nm by different samples were calculated for each sample. The results obtained are given in Table 2 and shown as a bar graph in Fig. 7.

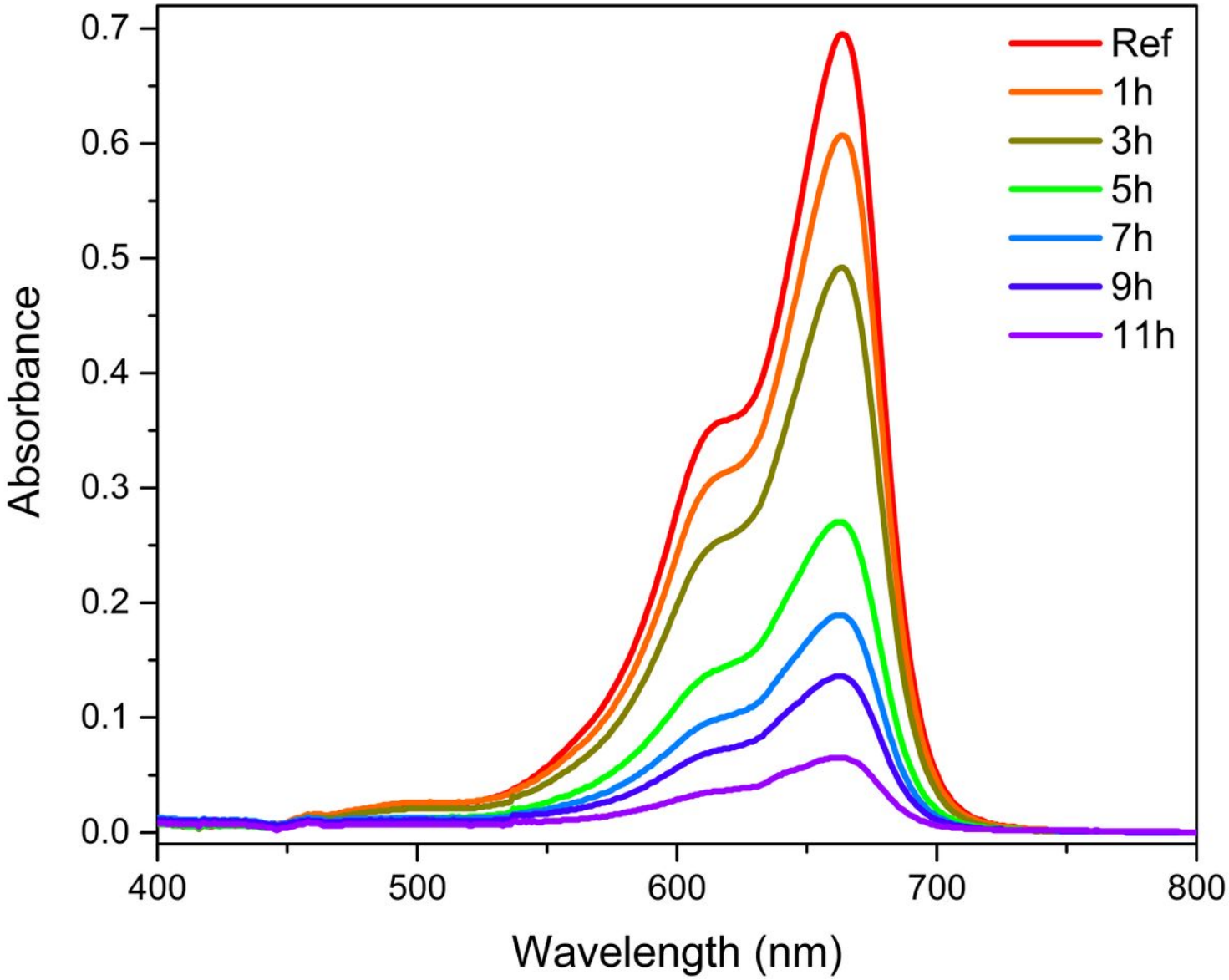

Figure 8

Absorption spectra of MB for sample S3 were drawn for different durations and are shown in Fig. 8.